

Reliability of laser-activated low-temperature polycrystalline silicon thin-film transistors

Du.-Zen Peng, Ting-Chang Chang, Hsiao-Wen Zan, Tiao-Yuan Huang, Chun-Yen Chang, and Po-Tsun Liu

Citation: [Applied Physics Letters](#) **80**, 4780 (2002); doi: 10.1063/1.1489096

View online: <http://dx.doi.org/10.1063/1.1489096>

View Table of Contents: <http://scitation.aip.org/content/aip/journal/apl/80/25?ver=pdfcov>

Published by the [AIP Publishing](#)

Articles you may be interested in

[Correlation of the generation-recombination noise with reliability issues of polycrystalline silicon thin-film transistors](#)

Appl. Phys. Lett. **85**, 311 (2004); 10.1063/1.1769073

[Effects of grain boundaries on performance and hot-carrier reliability of excimer-laser annealed polycrystalline silicon thin film transistors](#)

J. Appl. Phys. **95**, 5788 (2004); 10.1063/1.1699504

[Characteristics and stress-induced degradation of laser-activated low temperature polycrystalline silicon thin-film transistors](#)

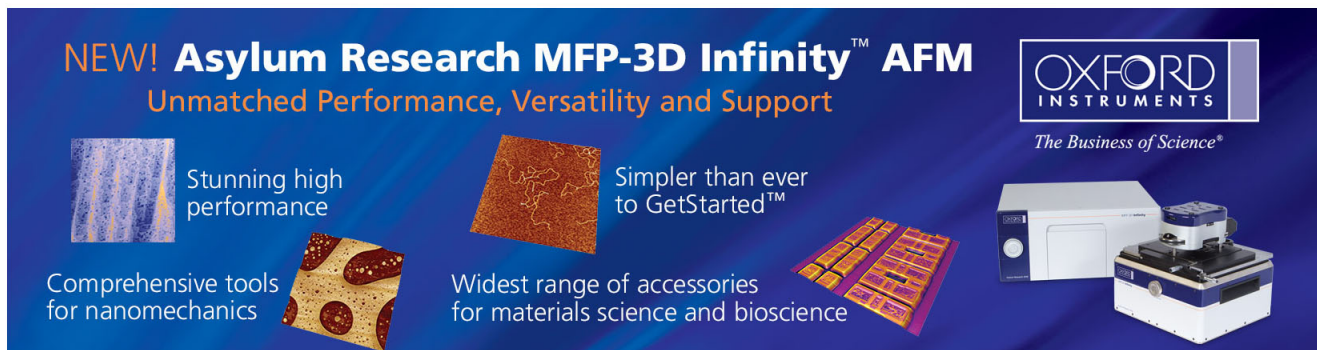
J. Appl. Phys. **93**, 1926 (2003); 10.1063/1.1535732

[Dimension scaling of low frequency noise in the drain current of polycrystalline silicon thin-film transistors](#)

J. Appl. Phys. **86**, 7083 (1999); 10.1063/1.371721

[Electrical and noise properties of thin-film transistors on very thin excimer laser annealed polycrystalline silicon films](#)

Appl. Phys. Lett. **74**, 3684 (1999); 10.1063/1.123221

The advertisement features a dark blue background with white and orange text. At the top left, it reads 'NEW! Asylum Research MFP-3D Infinity™ AFM' in large white letters, followed by 'Unmatched Performance, Versatility and Support' in orange. On the right, the Oxford Instruments logo is shown with the tagline 'The Business of Science®'. Below the text are four images: a textured surface, a circuit board, a grid of small components, and the MFP-3D Infinity AFM instrument itself. Text descriptions are placed around these images: 'Stunning high performance' next to the textured surface, 'Simpler than ever to GetStarted™' next to the circuit board, 'Comprehensive tools for nanomechanics' next to the grid, and 'Widest range of accessories for materials science and bioscience' next to the instrument.

Reliability of laser-activated low-temperature polycrystalline silicon thin-film transistors

Du.-Zen Peng

Institute of Electronics, National Chiao Tung University, Taiwan

Ting-Chang Chang^{a)}

Department of Physics, National Sun Yat-Sen University, Kaohsiung, Taiwan

Hsiao-Wen Zan, Tiao-Yuan Huang, and Chun-Yen Chang

Institute of Electronics, National Chiao Tung University, Taiwan

Po-Tsun Liu

National Nano Device Laboratory, 1001 Ta-Hsueh Rd. Hsin-Chu 300, Taiwan

(Received 24 January 2002; accepted for publication 25 April 2002)

In this letter, the characteristics and reliability of laser-activated polycrystalline silicon thin-film transistors (poly-Si TFTs) have been investigated by stressing the devices under $V_{ds}=12$ V and $V_{gs}=15$ V. In comparison with traditional furnace-activated poly-Si TFTs, the leakage current is relatively large for laser-activated poly-Si TFTs. Further, while the degradation rates of threshold voltage and subthreshold swing are comparable to those of traditional furnace-activated TFTs, the post-stress leakage and on/off current ratio for laser-activated poly-Si TFTs degrade much faster than those of furnace-activated counterparts. The laser activation modifies the grain structure between the drain and the channel region, and causes grain discontinuity extending from the drain to the channel region. As a result, an inferior reliability with extra trap state density and larger leakage current was observed in the laser-activated poly-Si TFTs. © 2002 American Institute of Physics. [DOI: 10.1063/1.1489096]

Polycrystalline silicon thin-film transistors (poly-Si TFTs) are attractive for many applications, such as the switching devices as well as peripheral driving circuits in the active matrix liquid crystal display.^{1,2} With a top-gate self-aligned TFT architecture, a solid phase crystallization or a laser crystallization is normally employed to crystallize the channel region, while a post-implant thermal anneal is traditionally used to activate the source/drain dopant.³ However, the post-implant thermal activation requires high temperature annealing, which is incompatible with low temperature processes on glass or even plastic substrates. In light of this, laser activation after self-aligned source/drain implant or gas immersion laser doping (GILD) has been proposed to replace the thermal activation anneal so as to reduce the maximum processing temperature.⁴ The self-aligned GILD method uses a laser to simultaneously incorporate and activate the dopant in the source/drain region. Excimer laser activation reduces not only the annealing temperature but also the resistivity of the source and drain regions, which helps improve the device turn-on characteristics, compared to traditional furnace activation. However, the reliability of laser-activated poly-Si TFTs, to the best of our knowledge, has not been carefully studied before.

In this letter, we compare $I-V$ characteristics and the reliability of poly-Si TFTs between laser activation and traditional post-implant furnace activation. It is found that laser activation results in larger leakage current and poorer reliability, which is believed to be due to extra trap state density generated near the drain side during laser activation. Al-

though no GILD is used in our experiment, we believe that similar results are expected for GILD method, which needs to be carefully taken into consideration for future low temperature poly-Si TFTs fabricated on plastic substrates.

Key fabrication steps of the laser-activated device are described as follows. Silicon wafers coated with a 500 nm thermal oxide were used as the starting substrates. An 80 nm undoped amorphous-Si(a-Si) layer was deposited by low-pressure chemical vapor deposition at 550 °C. The deposited a-Si layer was then laser-crystallized in vacuum at room temperature. The applied laser energy density for crystallization is 250 mJ/cm². After patterning and wet etching to define the active device island, a 50 nm gate oxide was deposited by plasma-enhanced chemical vapor deposition (PECVD) method. This was followed by the deposition and patterning of a 300 nm poly-Si gate layer. The gate electrode and source/drain regions were doped by phosphorus ions at a dosage of 5×10^{15} cm⁻², and an energy of 35 keV. Some wafers were then subjected to laser activation at room temperature. The laser for dopant activation was performed at an energy density of 200 mJ/cm². For comparison, wafers with traditional TFTs were also processed on the same run with the dopant activation by furnace annealing at 600 °C for 12 h in a nitrogen ambient instead. The measured resistivities were 1.41 mΩ cm and 2.43 mΩ cm for laser-activated (LA) and furnace-activated (FA) TFTs, respectively. This indicates that a significant reduction in source/drain resistance was indeed achieved by using laser activation method. Next, a 300-nm-thick oxide was formed as the cap layer by PECVD. Finally, contact hole definition and Al metallization were

^{a)}Electronic mail: tcchang@mail.phys.nsysu.edu.tw

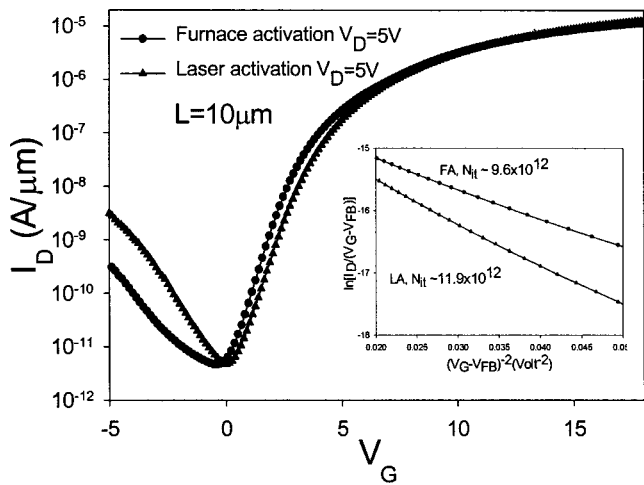


FIG. 1. Comparison of I_d-V_g characteristics between laser-activated and furnace-activated poly-Si TFTs. The inset plot compares the effective trap state density between LA and FA poly-Si TFTs.

performed, followed by a 400 °C sintering in nitrogen ambient for 30 min.

Figure 1 shows typical I_d-V_g characteristics of the LA and FA TFTs. While there is only slight difference in the turn-on characteristics such as threshold voltage and sub-threshold swing, the off-state leakage current ($V_g < 0$) is significantly larger for the laser-activated TFTs. The cause of the leakage current in TFTs is generally attributed to the drain electric field and the number of trap state density near the drain side.⁵⁻⁷ With nominally identical drain electric field in both LA and FA TFTs, a higher leakage current suggests that there is more trap state density near the drain side for the laser-activated TFTs. The inset plot of Fig. 1 shows the effective trap state density, extracted from the slope of $\ln[I_d/(V_g - V_{fb})]$ versus $(V_g - V_{fb})^{-2}$ characteristics⁸ for both LA and FA TFTs. A larger slope indicates a larger effective trap state density. We can see from the insert plot of Fig. 1 that TFTs with laser activation indeed have a larger effective trap state density. Figure 2 is the cross-sectional transmission electron microscopy (TEM) photo of a TFT after laser activation. It can be seen that there is modification of the grain structure extending from the drain to the chan-

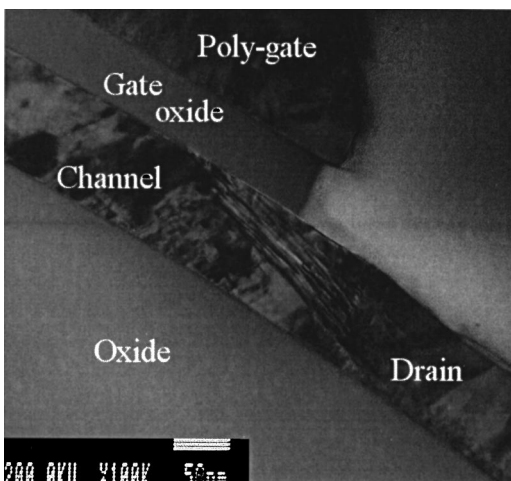


FIG. 2. Cross-sectional TEM photo of a laser-activated TFT. Note the lateral growth of grain structure near the drain side.

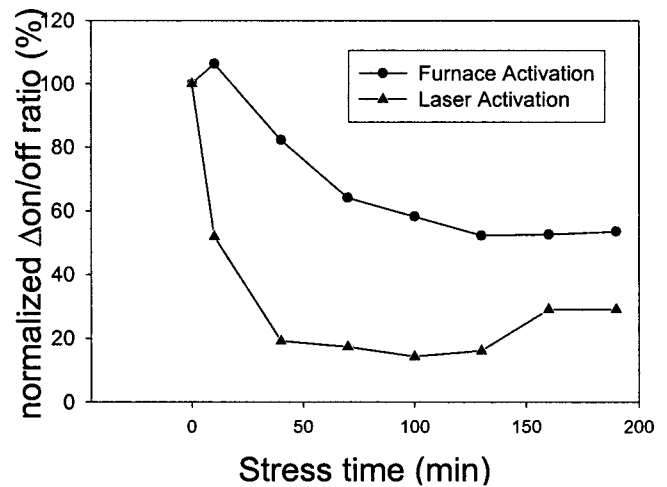


FIG. 3. Degradation rate of the on/off current ratio for laser- and furnace-activated poly-Si TFTs. The stress condition is $V_{ds} = 12$ V and $V_{gs} = 15$ V.

nel. During laser activation, the drain region is directly exposed to laser beam, while the channel region is shielded from the laser beam by the thick poly-gate lying on its top. Thus, while the drain region is already molten, the channel region remains relatively “cool.” With the existence of a lateral temperature gradient, the lateral growth of the grain results from the cool channel region stretching out to the molten drain region,⁹ as shown in Fig. 2. The discontinuity of the grain structure from the drain to the channel may therefore result in extra trap state density. From Figs. 1 and 2, we suggest that the extra trap state density is located near the drain side due to temperature gradient during laser activation.

Figure 3 depicts the degradation rate of the on/off current ratio after dc stress for LA and FA TFTs. The stress condition was chosen when the kink effect occurs at the output characteristics, i.e., $V_{ds} = 12$ V and $V_{gs} = 15$ V. It can be seen from Fig. 3 that the on/off ratio with laser activation degrades much faster than that with furnace activation. The aggravated degradation of the on/off ratio is due to the increased leakage current for LA TFTs. The extra trap state density near the drain side due to laser activation causes an accelerated degradation during stress, so even more trap state density is generated near the drain side after stress. To support this argument, we also examine two other device parameters, i.e., threshold voltage (V_{th}) and subthreshold swing (SS). Interestingly, no dramatic difference in degradation rate for V_{th} and SS are observed between LA and FA TFTs, as summarized in Table I. This indicates that under the stress condition, the extra trap density due to laser activation have little impact on channel and channel/oxide interface. This is

TABLE I. The degradation rates of threshold voltage (V_{th}) and subthreshold swing for laser- and furnace-activated TFTs. Both parameters were extracted at $V_{ds} = 0.1$ V.

	Time (h)			
	0	1	2	3
FA (V_{th})	0	+18%	+32%	+48%
LA (V_{th})	0	+21%	+30%	+27%
FA (SS)	0	+22%	+37%	+54%
LA (SS)	0	+32%	+43%	+46%

consistent with the hypothesis that the extra trap density due to laser activation causes more trap density only near the drain side after stress, and affects the device degradation characteristics such as increased post-stress leakage current.

In summary, we have examined the reliability of laser activation, particularly the post-implant laser activation for low-temperature poly-Si TFTs. Our results indicate that with laser activation, a larger leakage current results because of higher trap state density near the drain. In addition, laser-activated TFTs also degrade faster in terms of leakage current aggravation, due again to the higher trap state density near the drain. The cause of the increased trap state density is believed to be due to the drastic temperature gradient that exists between the drain and the channel region during laser activation, and may cause long-term stability problem for TFTs with laser activation.

The authors would like to acknowledge the financial support of the National Science Council (NSC) under Contract No. NSC 90-2215-E110-034.

- ¹H. Oshima and S. Morozumi, Tech. Dig. - Int. Electron Devices Meet., 157 (1989).
- ²S. D. Brotherton, *Semicond. Sci. Technol.* **10**, 721 (1995).
- ³J. B. Boyce, P. Mei, R. T. Fulks, and J. Ho, *Phys. Status Solidi A* **166**, 729 (1998).
- ⁴G. K. Giust and T. W. Sigmon, *IEEE Electron Device Lett.* **18**, 394 (1997).
- ⁵M. Yazaki, S. Takenaka, and H. Ohshima, *Jpn. J. Appl. Phys.* **31**, 206 (1992).
- ⁶C. F. Yeh, T. Z. Yang, C. L. Chen, T. J. Chen, and Y. C. Yang, *Jpn. J. Appl. Phys.* **32**, 4472 (1993).
- ⁷K. R. Olasupo and M. K. Hatalis, *IEEE Trans. Electron Devices* **8**, 1218 (1996).
- ⁸J. Levinson, F. R. Shepherd, P. J. Scanlon, W. D. Westwood, G. Este, and M. Ride, *J. Appl. Phys.* **53**, 1193 (1982).
- ⁹K. Shimizu, O. Sugiura, and M. Matsumura, *IEEE Trans. Electron Devices* **40**, 112 (1993).